JVI Journals.ASM.org

Two Distinct Sets of NS2A Molecules Are Responsible for Dengue Virus RNA Synthesis and Virion Assembly

Xuping Xie,[a] Jing Zou,[a,b] Chunya Puttikhunt,[c] Zhiming Yuan,[b] Pei-Yong Shi[a]

Novartis Institute for Tropical Diseases, Singapore[a]; State Key Laboratory of Virology, Wuhan Institute of Virology, Chinese Academy of Sciences, Wuhan, China[b]; Medical Biotechnology Unit, National Center for Genetic Engineering and Biotechnology, National Science and Technology Development Agency, Bangkok, Thailand[c]

ABSTRACT

Flavivirus nonstructural protein 2A (NS2A) plays important roles in both viral RNA synthesis and virion assembly. The molecular details of how the NS2A protein modulates the two distinct events have not been defined. To address this question, we have performed a systematic mutagenesis of NS2A using dengue virus (DENV) serotype 2 (DENV-2) as a model. We identified two sets of NS2A mutations with distinct defects during a viral infection cycle. One set of NS2A mutations (D125A and G200A) selectively abolished viral RNA synthesis. Mechanistically, the D125A mutation abolished viral RNA synthesis through blocking the N-terminal cleavage of the NS2A protein, leading to an unprocessed NS1-NS2A protein; this result suggests that amino acid D125 (far downstream of the N terminus of NS2A) may contribute to the recognition of host protease at the NS1-NS2A junction. The other set of NS2A mutations (G11A, E20A, E100A, Q187A, and K188A) specifically impaired virion assembly without significantly affecting viral RNA synthesis. Remarkably, mutants defective in virion assembly could be rescued by supplying in *trans* wild-type NS2A molecules expressed from a replicative replicon, by wild-type NS2A protein expressed alone, by a mutant NS2A (G200A) that is lethal for viral RNA synthesis, or by a different mutant NS2A that is defective in virion assembly. In contrast, none of the mutants defective in viral RNA synthesis could be rescued by *trans*-complementation. Collectively, the results indicate that two distinct sets of NS2A molecules are responsible for DENV RNA synthesis and virion assembly.

IMPORTANCE

Dengue virus (DENV) represents the most prevalent mosquito-borne human pathogen. Understanding the replication of DENV is essential for development of vaccines and therapeutics. Here we characterized the function of DENV-2 NS2A using a systematic mutagenesis approach. The mutagenesis results revealed two distinct sets of NS2A mutations: one set of mutations that result in defects in viral RNA synthesis and another set of mutations that result in defects in virion assembly. *trans*-Complementation analysis showed that mutants defective in viral RNA synthesis could not be rescued by wild-type NS2A; in contrast, mutants defective in virion assembly could be successfully rescued by wild-type NS2A or even by a mutant NS2A that is incompetent to support viral RNA synthesis. These results support a model in which two distinct sets of NS2A molecules are responsible for DENV RNA synthesis (located in the viral replication complex) and virion assembly (located in the virion assembly/budding site). The study confirms and extends our understanding of the two critical roles of flavivirus NS2A in viral RNA synthesis and virion assembly.

The *Flavivirus* genus within the *Flaviviridae* family contains many pathogens of public health importance, such as the four serotypes of dengue virus (DENV-1 to -4), yellow fever virus (YFV), West Nile virus (WNV), Japanese encephalitis virus (JEV), Saint Louis encephalitis virus (SLEV), and tick-borne encephalitis virus (TBEV) (1). DENV is prevalent in tropical and subtropical regions around the world. There are about 390 million human infections with DENV globally each year, with 96 million cases showing manifest symptoms (2). The World Health Organization has classified DENV as the most important mosquito-borne viral pathogen. Clinically, DENV infection causes a flu-like illness known as dengue fever (DF) and occasionally develops into an illness with potentially lethal complications known as dengue hemorrhagic fever (DHF) or dengue shock syndrome (DSS). No clinically approved vaccine or antiviral for the prevention of treatment of DENV infection is currently available. A better understanding of DENV replication at the molecular level is essential for vaccine and antiviral development.

Flavivirus virions are spherical to pleomorphic in shape and 40 to 60 nm in diameter (1). The flavivirus genome is a single-stranded, plus-sense RNA of 11 kb in length (3). The genomic RNA contains a 5′ untranslated region (UTR) with a type I cap structure, a single open-reading frame (ORF), and a nonpolyadenylated 3′ UTR (1). Upon entry into cells, the flavivirus genome is translated into a polyprotein by the cellular translation machinery. Co- and posttranslational processing by a combination of viral and cellular proteases generates three structural proteins (the capsid [C], premembrane [prM], and envelope [E] proteins) and seven nonstructural proteins (NS1, NS2A, NS2B, NS3, NS4A, NS4B, and NS5). Structural proteins are the components of the

Received 3 October 2014 **Accepted** 3 November 2014

Accepted manuscript posted online 12 November 2014

Citation Xie X, Zou J, Puttikhunt C, Yuan Z, Shi P-Y. 2015. Two distinct sets of NS2A molecules are responsible for dengue virus RNA synthesis and virion assembly. J Virol 89:1298–1313. doi:10.1128/JVI.02882-14.

Editor: K. L. Beemon

Address correspondence to Pei-Yong Shi, pei_yong.shi@novartis.com.

doi:10.1128/JVI.02882-14

virion. The nonstructural proteins form the viral replication complex, which is associated with the rearranged endoplasmic reticulum (ER) membranes (4). The glycoprotein NS1 plays an essential role in viral RNA replication (5). NS3 contains serine protease (using NS2B as a cofactor), RNA helicase, and nucleotide triphosphatase activities (6, 7). Besides enzymatic activities, NS3 is also involved in viral assembly through an unknown mechanism, which is independent of its enzymatic functions (8). The N-terminal one-third of NS5 harbors a methyltransferase activity and a weak guanylyltransferase activity, responsible for viral RNA cap formation and internal RNA methylation (9–12). The C-terminal two-thirds of NS5 is an RNA-dependent RNA polymerase (RdRp) (13). Other nonstructural proteins (NS2A, NS4A, and NS4B) contain transmembrane domains that are associated with the ER membrane. NS4A induces membrane rearrangement (14). NS4B forms a dimer (15), colocalizes with double-stranded RNA (dsRNA), and plays a critical role in viral replication (16). Besides viral replication, flavivirus nonstructural proteins also function in evasion of the host immune response (17–21).

NS2A (~22 kDa) is perhaps the least studied flavivirus protein. Biochemical analysis of DENV-2 NS2A suggested a membrane topology with five transmembrane segments (Fig. 1A) (22). After flavivirus polyprotein translation, the N terminus of NS2A is processed in the ER lumen by an unknown host protease (23), and the C terminus is cleaved in the cytoplasm by viral NS2B-NS3 protease. Three functions have been reported for flavivirus NS2A. (i) NS2A antagonizes the host immune response. The DENV and Kunjin virus (KUNV) NS2A proteins antagonize the interferon response (21, 24, 25); JEV NS2A blocks dsRNA-activated protein kinase PKR (26). (ii) NS2A functions in viral RNA synthesis. It colocalizes with viral double-stranded RNA in infected cells and interacts with the 3′ UTR of genomic RNA (27). (iii) NS2A functions in virion assembly. A K190S mutation of NS2A disabled YFV assembly (28); an I59N change of NS2A abolished the virion production of Kunjin virus (29); an R84A substitution of NS2A destroyed DENV-2 assembly (22). Despite the critical functions described above, the mechanisms of how NS2A participates in viral replication and assembly remain to be elucidated.

In this study, we performed a systematic mutagenesis of the flavivirus-conserved NS2A residues in DENV-2. Two distinct phenotypes were identified from the NS2A mutants. One mutant class was defective in viral RNA synthesis; mechanistic analysis showed that one such mutant (D125A) abolished viral RNA synthesis through blocking the cleavage at the NS1-NS2A junction. The other mutant class was defective in virion assembly. Remarkably, the NS2A mutants defective in virion assembly could be rescued by supplying in *trans* a wild-type (WT) NS2A from the replicative replicon of DENV, a wild-type NS2A protein alone, or a mutant NS2A (G200A) protein that is lethal for viral RNA synthesis. In contrast, the NS2A mutants defective in viral RNA synthesis could not be *trans*-complemented. The results clearly point to two distinct sets of NS2A that modulate flavivirus RNA synthesis and virion assembly.

MATERIALS AND METHODS

Bioinformatics. All amino acid sequences of NS2A proteins from DENV-1 to DENV-4, WNV, KUNV, JEV, SLEV, YFV, and TBEV were downloaded from the National Center for Biotechnology Information (NCBI) protein database. The alignment was performed using CLC Main Workbench software (CLC Bio).

Cell culture, viruses, and antibodies. Baby hamster kidney (BHK-21) cells were maintained in high-glucose Dulbecco modified Eagle medium (DMEM; Life Technologies) supplemented with 4 mM L-glutamine, 10% fetal bovine serum (FBS; HyClone Laboratories, Logan, UT), and 1% penicillin-streptomycin (Life Technologies). HEK293T (human embryo kidney 293T) cells were grown in low-glucose DMEM (Invitrogen) with 10% FBS and 1% penicillin-streptomycin. All cells were incubated at 37°C with 5% CO_2. A mouse monoclonal antibody (MAb) against enhanced green fluorescence protein (EGFP) was purchased from Roche. Rabbit IgG against EGFP was bought from Abcam. MAb 4G2 against the DENV envelope protein was prepared from hybridoma cell lines obtained from the American Type Culture Collection (ATCC). Rabbit anti-calnexin antibody and goat anti-mouse or anti-rabbit IgG conjugated to horseradish peroxidase (HRP) were purchased from Sigma-Aldrich. Alexa Fluor 488 and 568 goat anti-mouse IgG and Alexa Fluor 568 goat anti-rabbit IgG (Molecular Probes) were bought from Life Technologies. A mouse monoclonal antibody (D2C1) (30) against the dengue virus capsid protein was kindly provided by Chunya Puttikhunt.

Plasmid construction. Standard molecular biology methods were used in all plasmid constructions. The infectious clone pACYC-NGC FL (full length), replicon clone pACYC-NGC, subclone vector TA-D, pXJ-leader-EGFP, and pXJ-leader-NS2A-EGFP have been described before (22). For alanine scanning, all mutations were first introduced into subclone TA-D individually by using a QuikChange II XL site-directed mutagenesis kit (Agilent Technologies, Inc.). The DNA containing each mutation was inserted into the pACYC-NGC FL or pACYC-NGC replicon clone at the NheI and SacI restriction sites at DENV-2 nucleotide positions 2545 and 4343, respectively. For transient-expression constructs, the NS2A mutants were generated in pXJ-leader-NS2A-EGFP by site-directed mutagenesis. All constructs were confirmed by enzyme digests and DNA sequencing. The primer sequences used for mutagenesis are available upon request.

RNA transcription, electroporation, and virus production. Genome-length DENV-2 RNA was transcribed *in vitro*, using a T7 mMessage mMachine kit (Ambion, Austin, TX), from cDNA plasmid prelinearized by XbaI (engineered immediately downstream of the 3′ end of the viral genomic sequence). Ten-microgram RNA transcripts were electroporated into BHK-21 cells following a protocol described previously (31). After electroporation, cells were resuspended in DMEM containing 10% FBS and 1% penicillin-streptomycin and seeded in a T-75 or T-175 flask. At about 5 to 6 h posttransfection (p.t.), culture fluids were replaced with fresh medium to remove extracellular input RNAs. After incubation at 37°C for 24 h, cells were cultured in DMEM with 2% FBS at 30°C for another 4 days. On every day from day 1 to day 4 p.t., 500 μl of the supernatants was harvested, clarified by centrifugation at 500 × *g* for 5 min, and stored at −80°C. Extracellular viral titers were determined by plaque assay on BHK-21 cells.

Replicon transient-transfection assay. Ten-microgram WT or mutant replicon RNA transcripts were electroporated into BHK-21 cells. After electroporation, cells were seeded in a 12-well plate (2×10^5 cells/well). At 2, 4, 6, 24, 30, and 46 h p.t., cells were washed with phosphate-buffered saline (PBS) and lysed using lysis buffer (Promega). The plates containing the lysed cell samples were sealed and stored at −80°C. Once samples for all time points had been collected, luciferase signals were measured in a Clarity luminescence microplate reader (BioTek) according to the manufacturer's instructions.

Immunofluorescence assay (IFA). Cells were grown in an 8-well Lab-Tek chamber slide (Thermo Fisher Scientific). At given time points, cells were harvested, fixed in PBS supplemented with 4% paraformaldehyde at room temperature for 20 to 30 min, and permeabilized with 0.1% Triton X-100 in PBS at room temperature for 5 min. After 1 h of incubation in a blocking buffer containing 1% FBS in PBS, cells were treated with primary antibody for 1 h and washed with PBS three times for 5 min each time. The cells were then incubated with a secondary antibody (diluted 1:1,000) for 1 h in blocking buffer, after which the cells were washed as described

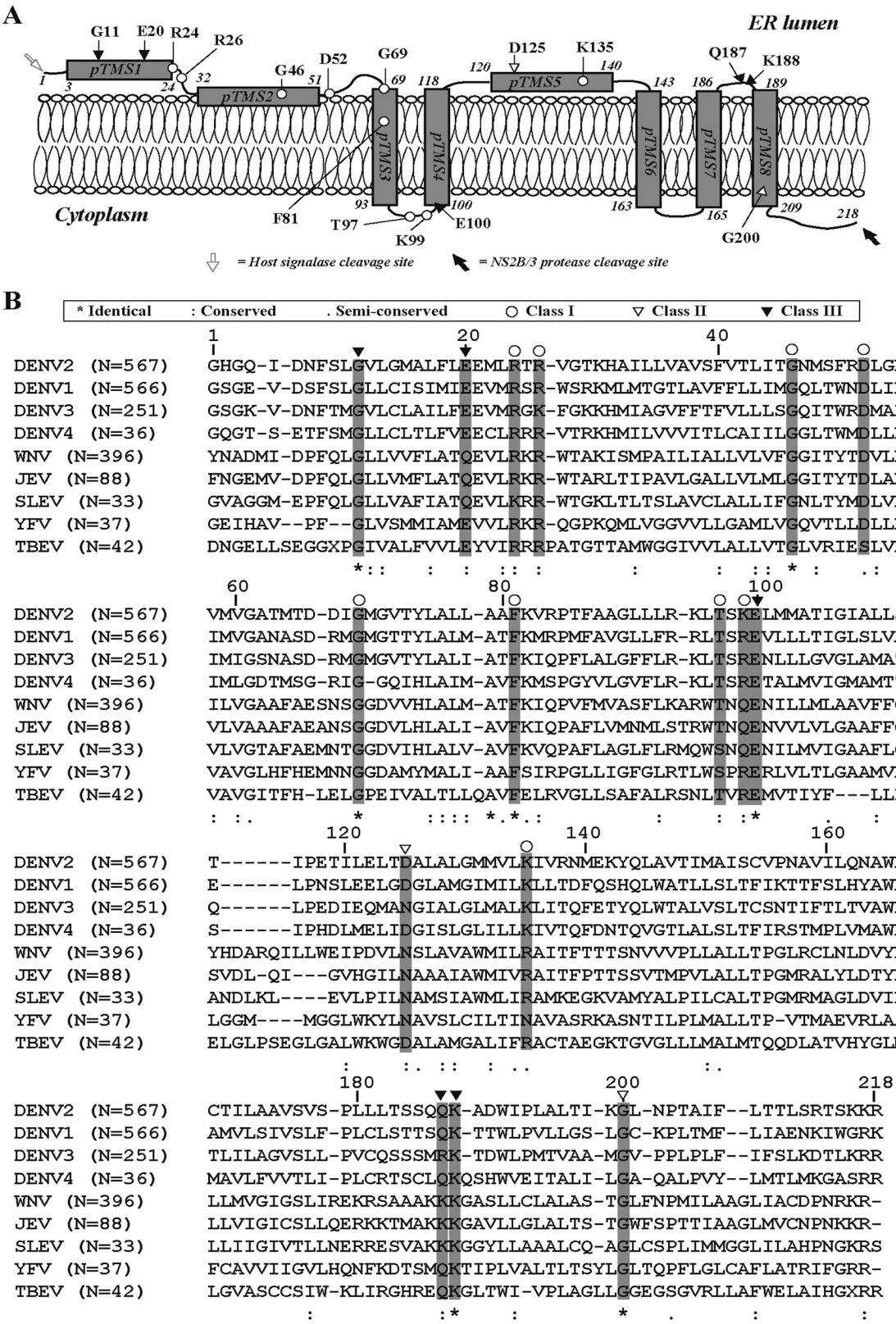

FIG 1 (A) Location of residues selected for mutagenesis in the membrane topology of NS2A. The topology of DENV-2 NS2A was adopted from our previous report (22). (B) Amino acid sequence alignment of NS2A proteins among flaviviruses. The numbers in parentheses show the numbers of NS2A amino acid sequences that were used for the alignment. The positions of amino acids in NS2A are labeled according to DENV-2 strain New Guinea C (NGC; GenBank accession number AF038403). The residues used for mutagenesis in this study are shaded. Symbols ○, ▽, and ▼ represent positions and original amino acids of the class I, II, and III alanine mutations, respectively.

above. Finally, the cells were mounted in a mounting medium with DAPI (4′,6-diamidino-2-phenylindole; Vector Laboratories, Inc.). Fluorescence images were taken with a Leica DM4000 B system. For confocal microscopy, fluorescence images were obtained by using a Zeiss LSM 510 Meta laser scanning confocal microscope (Biopolis Shared Facilities, Singapore). Images were processed using ImageJ software (NIH).

RT-PCR. Viral RNAs in culture fluids were extracted using a QIAamp viral RNA minikit (Qiagen). The intracellular viral RNAs from infected BHK-21 cells were isolated using an RNeasy minikit (Qiagen). Extracted RNAs were eluted in 50 μl RNase-free distilled water. For real-time reverse transcription-PCR (RT-PCR), two microliters of the RNA elution was used to quantify the RNA copy number using an iScript One-Step RT-PCR kit with SYBR green (Bio-Rad) and the primer pair NGC 7764V/NGC 7844C (22). Whole-genome sequencing was performed for all revertant isolates. For recombinant NS2A mutant viruses (produced from naive BHK-21 cells or derived from the *trans*-complementation experiment), fragments containing the NS2A region (from nucleotide positions 1787 to 4324 of the DENV-2 genome) were amplified, extracted, and sequenced.

DNA transfection, immunoprecipitation, SDS-PAGE, and Western blotting. HEK293T cells were transfected with 10 μg DNA in a 10-cm dish using the X-tremeGENE 9 DNA transfection reagent (Roche). At 48 h p.t., total cellular proteins were extracted by use of a radioimmunoprecipitation assay lysis buffer containing 50 mM Tris-HCl (pH 7.5), 150 mM NaCl, 1% Nonidet P-40 (NP-40), 0.5 % sodium deoxycholate, 0.1% sodium dodecyl sulfate (SDS), and EDTA-free protease inhibitor cocktail (Roche). EGFP fusion proteins were immunoprecipitated by mouse anti-EGFP MAb (Roche) following a protocol described previously (15). Protein samples were analyzed on a 12% SDS-polyacrylamide gel (Bio-Rad). Proteins were transferred onto a polyvinylidene difluoride (PVDF) membrane using a Trans-Blot apparatus (Bio-Rad), followed by incubation in blocking buffer (comprising 5% skim milk, 20 mM Tris-HCl, 137 mM NaCl, and 0.1% Tween 20) for 1 h. The blots were incubated in a blocking buffer containing a rabbit polyclonal antibody against EGFP (1:4,000 dilution; Abcam) overnight at 4°C. After three washes with Tris-buffered saline–Tween 20 (TBST), the blots were further incubated with a goat antirabbit antibody conjugated to horseradish peroxidase (1:30,000 dilution) in blocking buffer for 1 h. Finally, after four washes with TBST buffer, the antibody-protein complexes were detected using an ECL Western blotting system (GE Healthcare).

Selection of NS2A-EGFP BHK-21 cell line. pXJ-leader-NS2A-EGFP or pXJ-leader-NS2A mutant-EGFP plasmids (containing a neomycin resistance gene) were used for establishing cell lines persistently expressing WT or mutant NS2A-EGFP proteins. About 1×10^5 BHK-21 cells per well in a 6-well plate were transfected with 1 μg plasmids using the X-tremeGENE 9 DNA transfection reagent. At about 48 h p.t., G418 (Life Technologies) was added to a final concentration of 1 mg/ml. After every 2 to 3 days, the culture fluids were replaced with fresh medium containing 1 mg/ml G418. At about 2 weeks p.t., G418-resistant colonies were formed, harvested, and transferred into a 24-well plate. After another 2 days of incubation, cells were transferred to a T-75 flask for further expansion in medium containing 1 mg/ml G418. The cell lines were characterized by fluorescence microscopy and Western blot analysis using mouse anti-EGFP IgG.

RESULTS

Alanine scanning of flavivirus-conserved residues in NS2A protein. We performed an alanine scanning of amino acids that are conserved among flavivirus NS2A proteins using an infectious cDNA clone of DENV-2. Sequence alignment of the NS2A proteins of various flaviviruses revealed 8 identical amino acids, 36 conserved amino acids, and 10 semiconserved amino acids (Fig. 1B). We selected 16 residues for alanine scanning mutagenesis: (i) all 7 nonalanine residues that are identical among flavivirus NS2A proteins (G11, G46, G69, F81, E100, K188, and G200), (ii) conserved charged and polar residues (E20, R24, R26, T97, K99, D125, and Q187), and (iii) semiconserved charged residues (D52 and K135). The charged residues in the last two groups were selected because they are likely to participate in intra- or intermolecular interactions. The selected residues were individually mutated to alanine in the context of DENV-2 genome-length RNA. To examine the effect of mutations on viral replication, we electroporated equal amounts of wild-type (WT) and mutant genome-length RNAs into BHK-21 cells. Over several days p.t., the transfected cells were examined by IFA for viral RNA replication and the spread of viral infection, and virus production was determined by plaque assay on BHK-21 cells. On the basis of the replication phenotypes, those 16 NS2A mutants could be categorized into three different classes (Table 1).

TABLE 1 Summary of three classes of NS2A mutants with distinct phenotypes

Class	NS2A mutations	Phenotype
I	R24A, R26A, G46A, D52A, G69A, F81A, T97A, K99A, K135A	Viral replication is partially or not affected
II	D125A, G200A	RNA synthesis is defective
III	G11A, E20A, E100A, Q187A, K188A	Mutants are competent in viral RNA synthesis but incompetent in virion assembly

Class I mutants showed weak effects on viral replication. Nine of the 16 alanine mutants (the R24A, R26A, G46A, D52A, G69A, F81A, T97A, K99A, and K135A mutants) retained viral replication, although some of the mutants replicated less efficiently than WT virus (Fig. 2). These mutants were grouped as class I. Figures 2A and B, respectively, show the IFA and plaque morphologies of three representatives from the class I mutants (the R24A, G69A, and K99A mutants). Compared with cells transfected with WT RNA, cells transfected with the mutant RNAs generated comparable amounts of viral E protein-positive cells from days 1 to 4 p.t. (Fig. 2A); the mutant viruses formed plaques similar in size to or smaller than those formed by WT virus (Fig. 2B); cells transfected with mutant RNAs produced viral titers that were less than 100-fold lower than those of cells transfected with WT RNA (Fig. 2C). Sequencing of the mutant viruses (harvested on day 5 p.t.) confirmed that the engineered mutations were retained, with no other mutations occurring. Similar results were obtained for the other class I mutants (data not shown). Because class I mutants did not exhibit lethal phenotypes, they were not further analyzed in this study.

Class II mutants were defective in viral RNA synthesis. Mutation D125A or G200A impaired viral RNA synthesis. These two mutants were categorized as class II. Compared with cells transfected with WT RNA, cells transfected with class II mutant genome-length RNAs produced fewer E-positive cells from days 1 to 4 p.t. (Fig. 3A). However, both the D125A and G200A mutants yielded plaques similar to those of the WT virus (Fig. 3B); sequencing of the viruses (harvested on day 5 p.t.) showed that the engineered D125A and G200A mutations were reverted to the wild-type D125 and G200, respectively (Fig. 3C), indicating that the recovered infectious viruses were true revertants. These results suggest that the D125A or G200A substitution is lethal for viral replication.

We introduced the class II mutations into a DENV-2 replicon

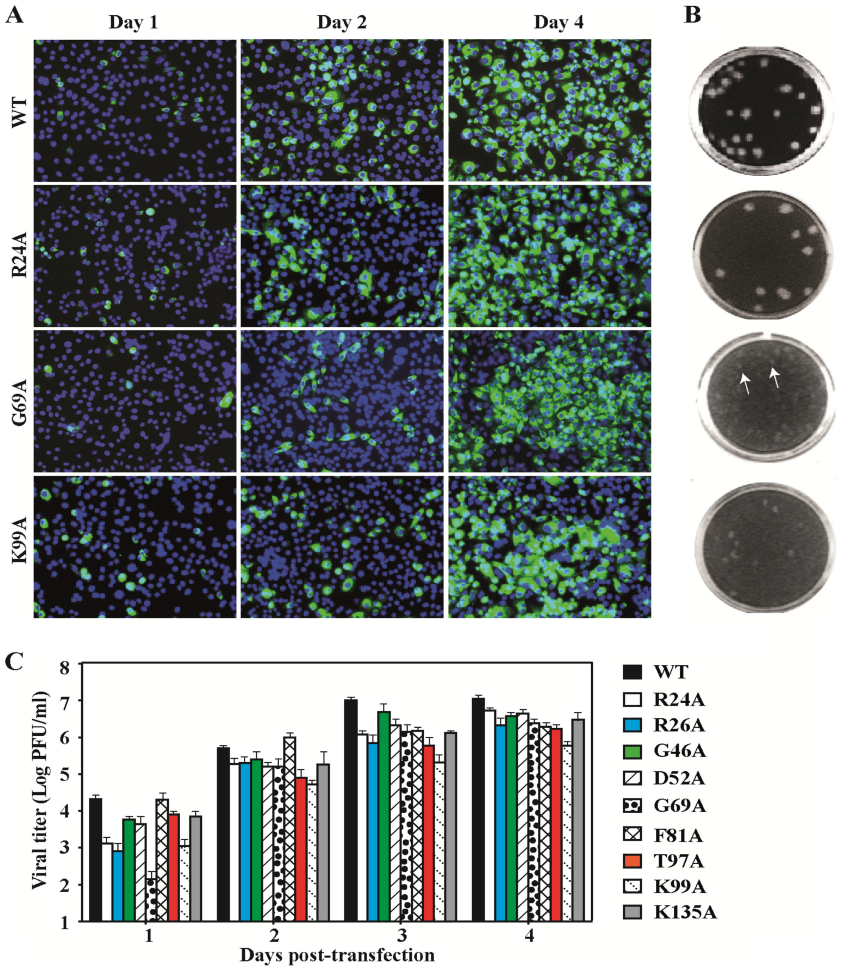

FIG 2 Characterization of class I mutants. (A) IFA. BHK-21 cells were electroporated with DENV-2 WT strain New Guinea C or individual NS2A mutant genome-length RNAs. From days 1 to 4 p.t., E protein was probed with the 4G2 antibody. Blue and green, nucleus and E-protein staining, respectively. (B) Plaque morphologies. Plaques were developed on day 5 postinfection. Arrows indicate opaque and small plaques. (C) Virus production. At the given time points, culture fluids were harvested and examined by plaque assay for determination of viral titers. The data show the mean values from two independent experiments performed in triplicate. Error bars show the standard deviations. The limit of detection of the plaque assay is 10 PFU/ml.

with a luciferase reporter gene (Fig. 3D, top) to confirm the results obtained with genome-length RNA described above. WT and mutant replicon RNAs were electroporated into BHK-21 cells. As shown in Fig. 3D (bottom), the class II mutant and WT replicons generated equivalent luciferase signals at 2, 4, and 6 h p.t. (representing times of viral RNA translation), demonstrating that these mutations do not affect viral protein translation. In contrast, at 24, 30, and 46 h p.t. (representing times of viral RNA synthesis), both D125A and G200A mutant replicons yielded luciferase signals similar to those of a previously reported nonreplicative replicon containing an NS4B K143A mutation (15). Collectively, the results demonstrate that class II mutants are defective in viral RNA synthesis.

Class II mutant D125A destroys viral RNA synthesis through abolishing NS1-NS2A cleavage. The cleavage of the NS1-NS2A junction is mediated by an unknown membrane-bound host protease in the ER. Previous studies showed that about 70% of the N-terminal NS2A is required for efficient NS1-NS2A cleavage (23). To examine whether mutations in NS2A affect its N-terminal processing, we used plasmid pXJ-leader-NS2A-EGFP (22) to transiently express an EGFP-tagged WT or mutant NS2A-EGFP protein. The leader sequence (containing the C-terminal 24 amino acids of the E protein, the N-terminal 50 amino acids of the NS1 protein, and the C-terminal 50 amino acids of NS1) was fused to the N terminus of NS2A to ensure the correct membrane topology of the protein. An EGFP was fused to the C terminus of the construct to facilitate NS2A detection because no NS2A antibody is currently available (Fig. 3E, top). The fused proteins were transiently expressed in HEK293T cells, immunoprecipitated by mouse anti-EGFP IgG, and probed with rabbit IgG against EGFP. As expected, the WT leader-NS2A-EGFP was completely processed to NS2A-EGFP, which migrated at the 36-kDa position (Fig. 3E, bottom left). The G200A mutation had no effect on the processing of leader-NS2A-EGFP. In contrast, mutant D125A generated a protein migrating at about 50 kDa, corresponding to the molecular mass of uncleaved leader-NS2A-EGFP; the alternative D125N or D125P mutation also abolished the cleavage of the NS1-NS2A junction (Fig. 3E, bottom right).

To exclude possible artifacts caused by the modified leader

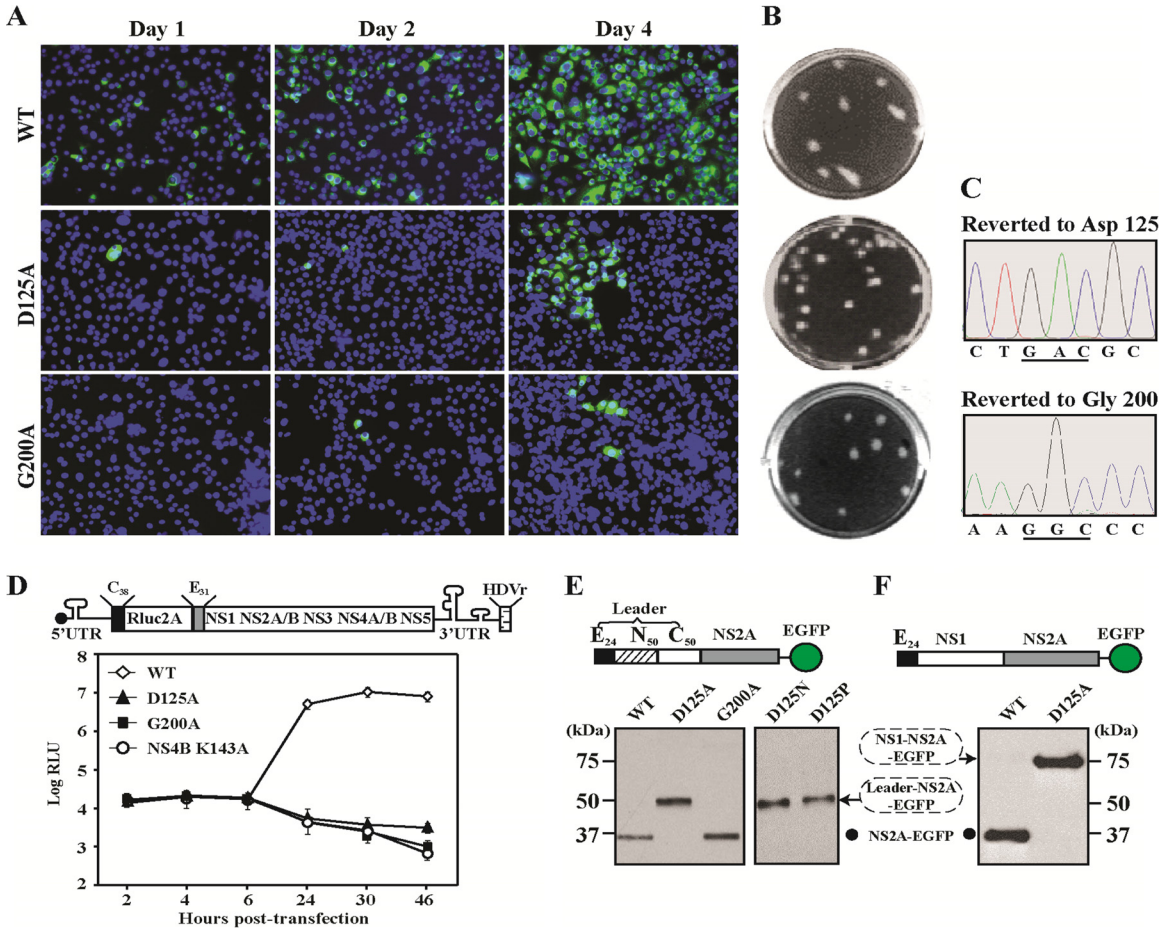

FIG 3 Characterization of class II mutants. (A) IFA. BHK-21 cells were electroporated with WT, D125A, or G200A genome-length RNAs. E-protein expression was monitored by the use of MAb 4G2 (green). (B) Plaque morphologies. (C) Chromatography of viral genome sequencing. On day 5 p.t., extracellular viral RNAs were extracted and used for RT-PCR, followed by DNA sequencing. The nucleotide sequences of Asp125 and Gly200 are underlined. (D) Replicon transient-transfection assay. (Top) Schematic diagram of the DENV-2 replicon with a *Renilla* luciferase gene (Rluc) fused with a 2A protease gene derived from foot-and-mouth disease virus (Rluc2A) (22). HDVr represents the hepatitis delta virus ribozyme sequence. Equal amounts of replicon RNAs (WT or mutant) were electroporated into BHK-21 cells. (Bottom) Luciferase signals were measured at the given time points. A nonreplicative replicon containing an NS4B K143A mutation (15) was included as a negative control. Each data point is the average from three replicates, and error bars show the standard deviations ($n = 3$). RLU, relative light units. (E) Analysis of the cleavage at the NS1-NS2A junction in the context of leader-NS2A-EGFP. (Top) Schematic diagram of leader-NS2A-EGFP in pXJ plasmids (22). The leader sequence contains a signal peptide derived from the last 24 residues of E protein (E_{24}), the first 50 residues of NS1 (N_{50}), and the last 50 residues of NS1 (C_{50}). (Bottom) HEK293T cells were transfected with plasmid carrying leader-NS2A (WT, D125A, G200A, D125N, or D125P)-EGFP. At 48 h p.t., EGFP fusion proteins were precipitated, separated by SDS-PAGE, and detected by Western blotting using a rabbit IgG against EGFP. The sizes of protein standards are shown on the left. (F) Analysis of the cleavage at the NS1-NS2A junction in the context of NS1-NS2A-EGFP. (Top) Construction of E_{24}-NS1-NS2A-EGFP in plasmid pXJ. (Bottom) HEK293T cells were transfected with a plasmid carrying E_{24}-NS1-NS2A (WT or D125A)-EGFP. At 48 h p.t., EGFP fusion proteins were immunoprecipitated and detected using the same protocol described in the legend to panel E.

sequence containing an incomplete NS1, we examined the D125A mutation in the context of E_{24}-NS1-NS2A-EGFP (including the last 24 amino acids of E [E_{24}] and full-length NS1; Fig. 3F, top). EGFP fusion proteins were immunoprecipitated and analyzed by Western blotting using an EGFP antibody. WT E_{24}-NS1-NS2A-EGFP was completely cleaved to yield NS2A-EGFP (Fig. 3F). In contrast, D125A mutant E_{24}-NS1-NS2A-EGFP generated a protein migrating at 75 kDa, corresponding to the size of uncleaved NS1-NS2A-EGFP (Fig. 3F). Collectively, the results demonstrate that an NS2A mutation, located far downstream of the NS1-NS2A cleavage site, could abolish the N-terminal process of NS2A, leading to a complete loss of viral RNA synthesis.

Class III mutants significantly reduce virus assembly. Transfection of class III mutant genome-length RNAs (G11A, E20A, E100A, Q187A, and K188A RNAs) generated E-positive cells equivalent in number to the number of E-positive cells generated after transfection with WT RNA at day 1 p.t. (Fig. 4A). From day 1 to day 4 p.t., the number of E-positive cells among the WT RNA-transfected cells increased, whereas fewer E-positive cells were observed among the mutant RNA-transfected cells (Fig. 4A), suggesting a decreased spread of viral infection in the mutant RNA-transfected cells. The decline in the number of E-positive cells from day 1 to day 4 p.t. is due to a cytopathogenic effect mediated by cumulative viral RNA replication and protein translation in the mutant RNA-transfected cells. Culture fluids harvested from the mutant RNA-transfected cells were examined for virus production by plaque assay. No plaques developed after incubation for 6 days for any of the class III mutants (data not

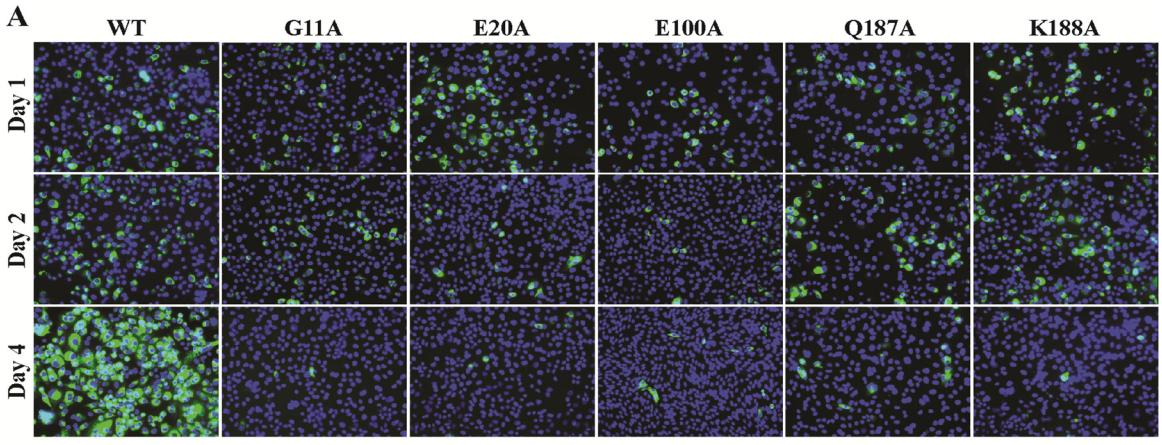

C

Day p.t.	WT	G11A	E20A	E100A	Q187A	K188A
2	$(3.2 \pm 0.2) \times 10^4$	<10	<10	<10	345 ± 68	<10
3	$(8.1 \pm 0.4) \times 10^6$	10 ± 20	20 ± 18	50 ± 22	2970 ± 120	<10
4	$(1.5 \pm 0.5) \times 10^7$	50 ± 25	85 ± 55	150 ± 35	3,250 ± 280	<10

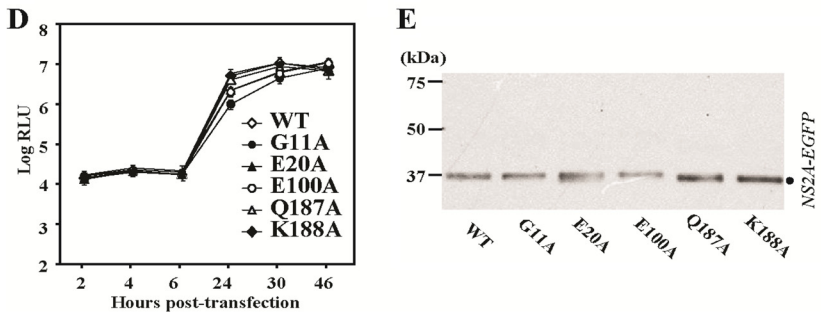

FIG 4 Characterization of class III mutants. (A) After electroporation of BHK-21 cells with WT or individual class III mutant genome-length RNAs on days 1 to 4 p.t., E protein was monitored by use of the 4G2 antibody (green). Representative images are shown. On days 2, 3, and 4 p.t., supernatants were harvested, clarified, and used to infect naive BHK-21 cells in an 8-well chamber slide. (B) At 48 h postinfection at 30°C, cells were fixed and examined by use of the D2C1 antibody for capsid protein expression. Capsid-positive cells were counted. Representative images are shown. (C) The average viral titers (IFU/ml) and standard deviations of three independent measurements are shown. (D) Replicon transient-transfection assay. Equal amounts of WT or class III mutant replicon RNAs were electroporated into BHK-21 cells. Luciferase signals were measured at the given time points. The averages and standard deviations from three replicates are shown. (E) Analysis of the cleavage at the NS1-NS2A junction in the context of leader-NS2A-EGFP. HEK293T cells were transfected with plasmids carrying leader-NS2A (WT or individual class III mutant)-EGFP. At 48 h p.t., EGFP fusion proteins were immunoprecipitated and detected.

shown). To further examine whether there were any infectious virus particles in the culture fluids after electroporation, we performed IFA analysis on naive BHK-21 cells that had been infected with the culture fluids harvested from day 2 to day 4 posttransfection. Counting the capsid-positive cells allowed us to estimate the number of infectious-forming units (IFU) for each of the class III mutants. Interestingly, all class III mutants except the K188A mutant could generate capsid-positive cells (Fig. 4B), albeit at varied efficiencies. As shown in Fig. 4C, on day 4 p.t., Q187A RNA generated at most 3,250 IFU/ml viruses; G11A, E20A, and E100A RNA produced about 50 to 150 IFU/ml viruses; in contrast, WT RNA generated about 1.5×10^7 IFU/ml virus. Quantitative RT-PCR analysis further demonstrated that the class III mutant RNA produced 10^4-fold less extracellular viral RNA than the WT RNA (data not shown). To exclude the possibility that the observed virus production was due to revertants, we extracted intracellular RNAs from the infected naive BHK-21 cells and sequenced the whole genome. The sequencing results confirmed that the engineered class III mutations were retained without any other mutations (data not shown).

To examine the effect of class III mutations on viral RNA synthesis, we analyzed these mutations in the DENV-2 luciferase repli-

con. As shown in Fig. 4D, the luciferase signals of the G11A, E20A, and E100A mutants decreased to 45%, 70%, and 69% of the WT signal, respectively, at 24 h p.t.; no significant difference in luciferase activity was observed between the mutant and WT replicons at 30 and 46 h posttransfection. The results indicate that class III mutations have only a marginal effect on viral RNA synthesis.

To examine whether class III mutations affect the cleavage of NS1-NS2A, we introduced individual mutations into plasmid pXJ-leader-NS2A-EGFP and examined the cleavage at the NS1-NS2A junction as described above. All class III mutants as well as the WT construct generated fully cleaved NS2A-EGFP products (Fig. 4D), suggesting that class III mutations do not affect the processing of NS1-NS2A. Notably, mutant E100A NS2A-EGFP migrated slightly more slowly than the WT and other mutants (Fig. 4D); the nature of this aberrant migration is currently not understood. Nevertheless, the data indicate that class III mutations do not affect the processing of NS1-NS2A.

Mutant K188A can be partially *trans*-complemented in a DENV-2 replicon cell line. We tested whether the defects in viral RNA synthesis and virion assembly could be *trans*-complemented in a DENV-2 replicon BHK-21 cell line (BHK-21 Rep) (31). Since the Q187A mutant retained a moderate level of virion formation (Fig. 4C), this mutant was excluded from the following *trans*-complementation analysis. Figure 5A shows a flowchart of the *trans*-complementation experiment. Genome-length RNAs containing individual NS2A mutations were electroporated into BHK-21 Rep cells. On days 1 to 4 p.t., cells were monitored by IFA for expression of the E protein (which could be expressed only from the genome-length RNA and not the replicon). A notable increase in E-positive cells among K188A mutant-transfected cells was observed from days 1 to 4 p.t. (Fig. 5B), indicating the limited spread of mutant virus infection in the replicon cells. To directly show that infectious viruses (containing the class III genome-length mutant RNAs) were produced, we infected naive BHK-21 cells with culture fluids collected on day 4 p.t.; viral capsid-positive cells were observed in the infected naive BHK-21 cells (Fig. 5C). The mutant RNAs generated about 48 to 2,000 IFU/ml infectious viruses from the BHK-21 Rep cells (Fig. 5D). Comparison of the viral titers derived from naive BHK-21 cells (Fig. 4C) and those derived from BHK-21 Rep cells (Fig. 5D) suggests that only mutant K188 was successfully *trans*-complemented to improve virion production.

To exclude the possibility that the observed *trans*-complementation was due to reversion of the NS2A mutation, we extracted intracellular RNAs from the infected naive BHK-21 cells shown in Fig. 5C and selectively sequenced the NS2A gene derived from the genome-length RNA (using a primer pair targeting E [nucleotide position 1794] and NS2B [nucleotide position 4324]); the sequencing results confirmed that the engineered class III substitutions were retained without any other mutations (Fig. 5E). Further passaging of the culture fluids of cells from Fig. 5C on new naive BHK-21 cells did not yield any E-positive cells (data not shown). Overall, the results presented above suggest that the class III K188A mutant can be partially *trans*-complemented in a DENV-2 replicon cell line. It is currently not known why the efficiency of virion assembly of other class III mutants could not be significantly improved in the replicon cells.

Next, we asked whether the RNA synthesis defect of class II mutants (the D125A and G200A mutants) could be *trans*-complemented in the replicon BHK-21 cells. After electroporation of D125A genome-length RNA into the replicon cells, no E-positive cells were observed (Fig. 5B); incubation of naive BHK-21 cells with the culture fluids from the cells shown in Fig. 5B did not produce any capsid-positive cells (Fig. 5C); in addition, RT-PCR of the culture fluids of cells from Fig. 5B on day 4 p.t. was also negative for the detection of viral RNA (data not shown). For mutant G200A, several E-positive cells were detected after the mutant genome-length RNA was electroporated into the replicon cells on days 3 and 4 p.t. (Fig. 5B); the culture fluids harvested on day 4 p.t. contained a few infectious viral particles (Fig. 5C and D); however, sequencing of the RNA from culture fluids of cells from Fig. 5B and C showed that the engineered G200A mutation reverted to Asp (Fig. 5B, bottom right) and subsequently to wild-type Gly (Fig. 5E), respectively. These data suggest that the class II mutations D125A and G200A, which abolish viral RNA synthesis, cannot be *trans*-complemented by the replication complex supplied in the replicon cells.

NS2A alone can rescue the virus assembly defects of class III mutants. To determine whether NS2A alone could rescue the defects of NS2A mutants, we established a BHK-21 cell line that stably expressed the NS2A-EGFP protein using plasmid pXJ-leader-NS2A-EGFP containing a neomycin resistance gene. Figure 6A shows the procedures used to generate the NS2A-GFP-expressing cell line. All selected cells were EGFP positive (Fig. 6B, left). The EGFP signal displayed an ER-like distribution pattern (Fig. 6B, right), which was further supported by colocalization with calnexin, an ER marker protein (Fig. 6C). Western blot analysis by an EGFP antibody showed a dominant 36-kDa band (representing processed NS2A-EGFP), a weak 72-kDa band (possibly representing a dimer of NS2A-EGFP), and several faint 75- to 100-kDa bands (possibly representing higher oligomers of NS2A-EGFP) (Fig. 6D). The results indicate that NS2A-EGFP was correctly targeted to the ER membrane by its upstream leader, after which the leader was efficiently cleaved. The NS2A-EGFP signals were not lost after continuous culturing of the NS2A-expressing cells for 30 passages (for a total of 3 months; data not shown), suggesting that the NS2A-expressing cell line is stable.

We used the NS2A-expressing cell line to *trans*-complement class II and III mutant genome-length RNAs (Fig. 7). Remarkably, all class III mutants could be efficiently *trans*-complemented in the NS2A-EGFP-expressing cells. This was indicated by an increased number of E-positive cells posttransfection (Fig. 7A) and by successful infection of naive BHK-21 cells with the culture fluids harvested from the transfected cells (Fig. 7B). Sequencing of the intracellular viral RNA derived from the infected naive BHK-21 cells confirmed that the engineered mutations were retained in the genome-length RNAs (Fig. 7C), suggesting no reversion during the complementation experiment. On day 4 p.t., each of the class III mutants generated infectious viruses to 4.3×10^3 to 3.6×10^4 IFU/ml (Fig. 7D), demonstrating that the *trans*-complementation efficiency in the WT NS2A-EGFP-expressing cells is higher than that in BHK-21 Rep cells (compare Fig. 7D with Fig. 5D). The lower complementation efficiency in replicon cells could be due to the competition over viral replication (for limited host factors) between the replicon RNA and the mutant genome-length RNA, whereas no such superinfection exclusion (32) exists in NS2A-EGFP-expressing cells.

For class II mutants, no E-positive cells were observed after D125A genome-length RNAs were transfected into the WT NS2A-EGFP-expressing cells (Fig. 7A). However, several capsid-positive cells were detected after infecting naive BHK-21

A

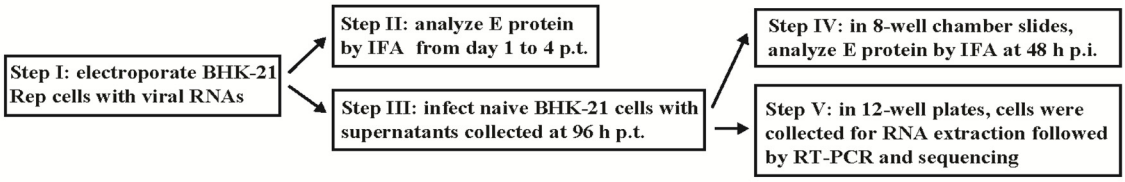

B

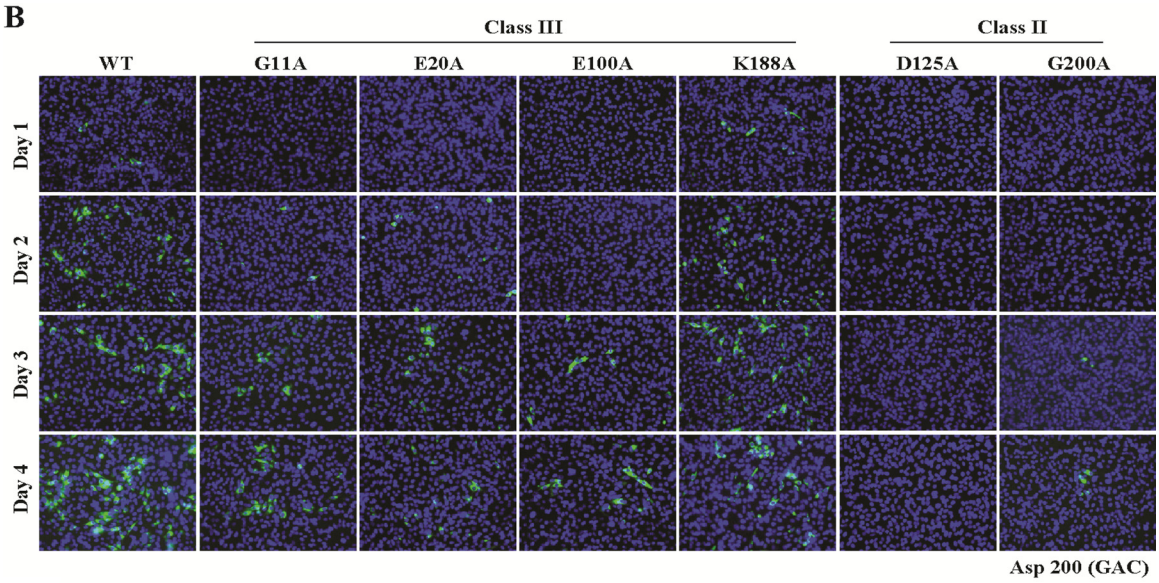

C

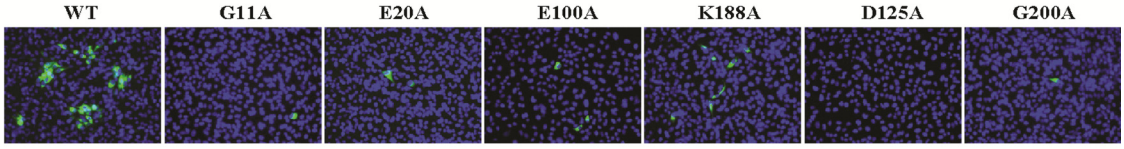

D

RNAs	WT	G11A	E20A	E100A	K188A	D125A	G200A
(IFU/ml)	$(5 \pm 0.2) \times 10^4$	48 ± 24	130 ± 30	182 ± 38	2,000 ± 358	N.D.	2 ± 2

E

Mutant RNAs	G11A	E20A	E100A	K188A	D125A	G200A
Viral sequencing	Ala11 (GCC)	Ala20 (GCC)	Ala100 (GCC)	Ala188 (GCC)	N.D.	Reverted to Gly200 (GGC)

FIG 5 *trans*-Complementation analysis using BHK-21 Rep cells. (A) Flowchart of *trans*-complementation analysis. (B) IFA analysis of transfected cells. BHK-21 Rep cells were electroporated with equal amounts (10 μg) of WT or individual mutant genome-length RNAs. From days 1 to 4 p.t., cells were fixed and analyzed for E-protein expression by IFA using 4G2 antibody (green). The nucleotide sequence of Asp200 identified by RT-PCR and cDNA sequencing of the recovered revertants is shown. (C) IFA analysis of infected cells for quantifying viral titers. On day 4 p.t., supernatants were harvested and used to infect naive BHK-21 cells. Capsid proteins in infected cells were detected by MAb D2C1 and Alexa Fluor 488 goat anti-mouse IgG (green). (D) Average viral titers and standard deviations (IFU/ml) from three independent measurements. N.D., not detected. (E) Viral genome sequencing. Intracellular viral RNAs were extracted from infected BHK-21 cells and subjected to RT-PCR and cDNA sequencing. The regions between E (nucleotide position 1794) and NS2B (nucleotide position 4324) were sequenced. The amino acid and nucleotide sequences at the corresponding positions are indicated.

cells with culture fluids from the transfected NS2A-EGFP-expressing cells (Fig. 7B). Sequencing of the intracellular viral RNA showed that the engineered D125A mutation reverted to the WT Asp (Fig. 7C). For the G200A mutant, few E-positive cells were detected among the transfected NS2A-EGFP-expressing cells on day 4 p.t. (Fig. 7A), and few capsid-positive cells were detected among the culture fluid-infected naive cells (Fig. 7B); sequencing of the viral RNAs derived from the IFA-positive cells from Fig. 7A and B showed that the engineered G200A mutation reverted to Asp (Fig. 7A, bottom right) and WT Gly (Fig. 7C), respectively. These results are similar to those observed for BHK-21 Rep cells, arguing that class II mutants, which are defective in viral RNA synthesis, cannot be *trans*-complemented by WT NS2A.

Class II mutant G200A can efficiently rescue the defect in virus assembly of class III mutants. The results presented above

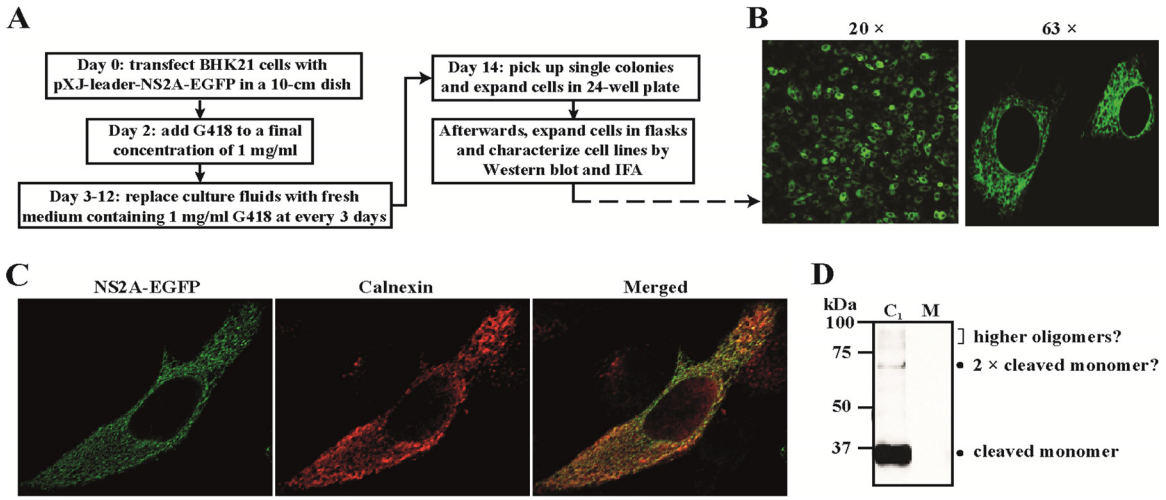

FIG 6 Selection of the NS2A-EGFP BHK-21 cell line. (A) Schematic diagram for selection of the NS2A-EGFP BHK-21 cell line. (B) Fluorescence microscopy analysis. EGFP signals were observed under a fluorescence microscope with a ×20 or a ×63 objective lens. (C) Confocal microscopy. NS2A-EGFP BHK-21 cells were fixed with 4% paraformaldehyde and permeabilized in 0.1% Triton X-100. Cells were probed with a rabbit antibody against calnexin, followed by Alexa Fluor 568 goat anti-mouse IgG. The green and red fluorescence was observed by use of a confocal microscope. Images were processed and merged using ImageJ software. (D) Expression of the EGFP fusion protein in the NS2A-EGFP BHK-21 cell line. Total intracellular proteins derived from NS2A-EGFP BHK-21 cells (lane C_1) or naive BHK-21 cells (lane M) were extracted and immunoprecipitated by a mouse anti-EGFP IgG, followed by Western blotting using rabbit anti-EGFP IgG.

prompted us to ask whether class II mutant NS2A (defective in viral RNA synthesis) could rescue the defect in virion assembly of class III mutants. To address this question, we established a cell line that stably expressed mutant G200A NS2A-EGFP. The D125A mutant was excluded in this study due to the complexity of uncleaved NS1-NS2A (Fig. 3E and F). Similar to WT NS2A (Fig. 6B), G200A NS2A-EGFP proteins showed an ER-resident pattern in cells in which they were stably expressed (Fig. 8A). Western blot analysis of the NS2A-expressing cell lines showed that the G200A mutation did not affect leader-NS2A cleavage, yielding a cleaved NS2A-EGFP with an expected size of 36 kDa, plus a few weak higher-molecular-mass bands possibly representing oligomers of NS2A-EGFP (Fig. 8B).

Next, we performed *trans*-complementation experiments by transfecting class III mutant genome-length RNAs into the NS2A (G200A)-EGFP-expressing cells. From days 2 to 4 p.t., the number of E-positive cells slightly increased after transfection with all class III mutant genome-length RNAs (Fig. 8C), suggesting the successful spread of viral infection. The presence of infectious viruses in culture fluids was confirmed by productive infection of naive BHK-21 cells (Fig. 8D). Strikingly, the infectious viral titers increased from days 2 to 4 p.t. for all class III mutants (Fig. 8E). On day 4 p.t., about 4,890 to 12,380 IFU/ml infectious viruses accumulated in the culture medium (Fig. 8E). The *trans*-complementation efficiencies of all class III mutant RNAs in NS2A (G200A)-EGFP-expressing cells were comparable to those in the WT NS2A-EGFP-expressing cells (Fig. 7D). Sequencing of the intracellular viral RNAs derived from the infected naive BHK-21 cells (Fig. 8D) confirmed that the engineered mutations were retained without any other mutations (data not shown). Collectively, the data demonstrate that class II mutant G200A NS2A can efficiently rescue the defect of virion assembly of class III mutants.

Class III mutants G11A and K188A can efficiently rescue the defect in virus assembly of each other. To test whether distinct class III mutants could *trans*-complement each other, we established four cell lines that stably expressed mutant G11A, E20A, E100A, or K188A NS2A-EGFP. All cells from the selected cell line were EGFP positive (Fig. 9A, four panels on the left). Similar to the WT NS2A (Fig. 6B), the G11A, E100A, and K188A NS2A-EGFP proteins showed an ER-resident pattern in cells stably expressing the mutations (data not shown). In contrast, large EGFP puncta in E20A NS2A-EGFP-expressing cells could be observed under a fluorescence microscope (Fig. 9A, right), suggesting that E20A NS2A-EGFP may fold incorrectly and, consequently, form intracellular aggresomes. Such a mechanism might account for its defect in viral assembly (Fig. 4). Western blot analysis of the mutant-expressing cell lines showed that none of these mutations affected leader-NS2A cleavage (data not shown), which agrees with the findings of transient-expression analysis (Fig. 4E).

Next, we applied these cells to *trans*-complementation of class III mutants (the G11A, E20A, E100A, and K188A mutants). Each of the cell lines was electroporated with equal amounts of individual mutant genome-length RNA. IFA (for monitoring of E-positive cells) showed virus spreading in G11A NS2A-expressing cells transfected with K188A RNA and in K188A NS2A-expressing cells transfected with G11A RNA (Fig. 9B to E), suggesting that successful *trans*-complementation occurs between G11A and K188A mutant NS2A molecules. However, the IFA results did not yield observable virus spreading when other mutant combinations were used. Quantification of the extracellular viruses by infection of naive BHK-21 cells using culture fluids harvested on days 2 to 4 p.t. further confirmed that the G11A/K188A combination produced much higher titers than other mutant combinations (Fig. 9F). Three other combinations (E20A RNA in K188A NS2A-expressing cells, E100A RNA in G11A NS2A-expressing cells, and E100A RNA in K188A NS2A-expressing cells) generated viral titers greater than 100 IFU/ml (Fig. 9F). Overall, the results indicate that distinct combinations of two class III NS2A mutants can *trans*-complement to restore virion assembly.

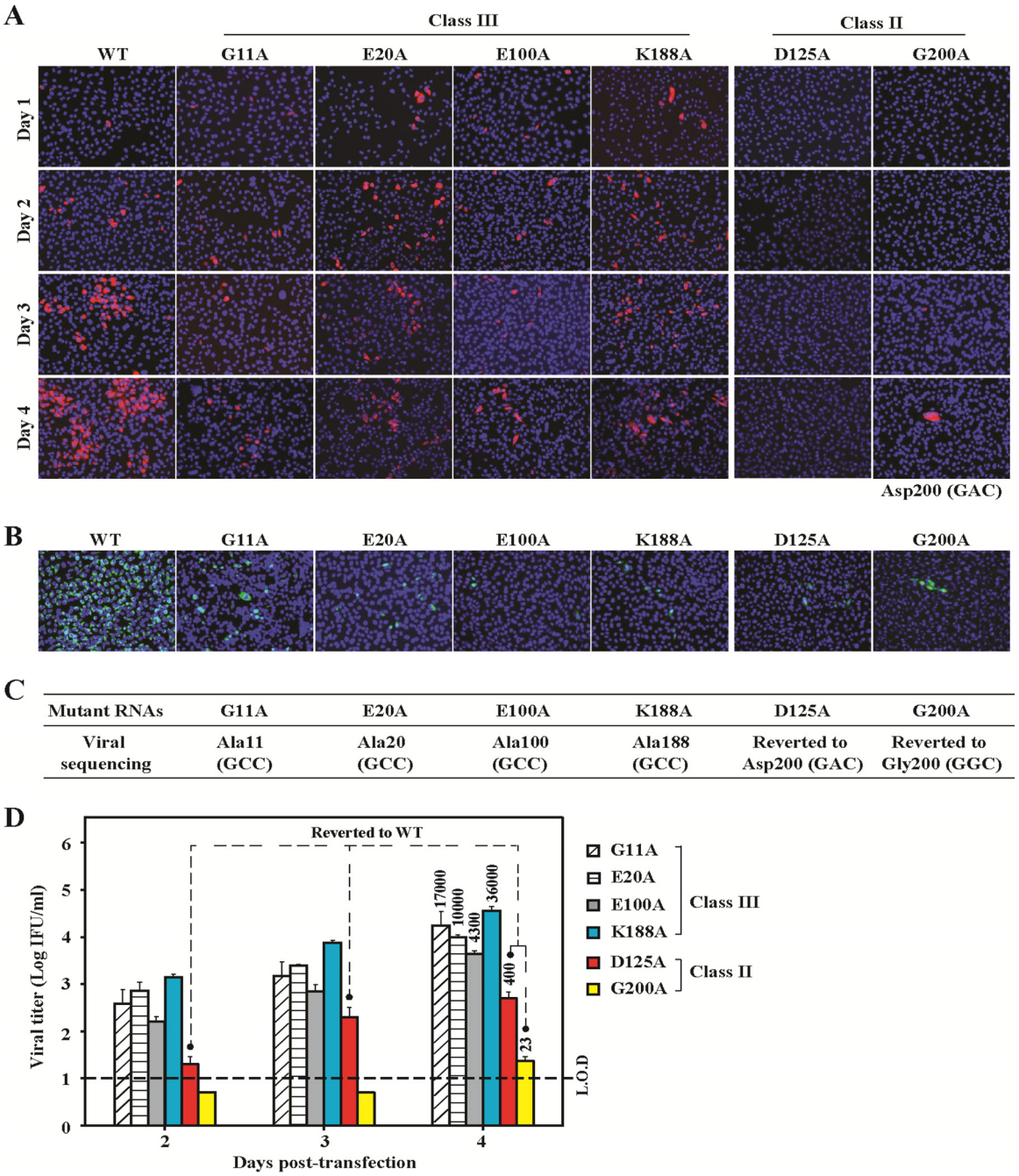

FIG 7 *trans*-Complementation analysis using NS2A-EGFP BHK-21 cells. (A) NS2A-EGFP BHK-21 cells were electroporated with equal amounts (10 μg) of WT or individual mutant genome-length RNAs. From days 1 to 4 p.t., E proteins were detected using MAb 4G2, followed by Alexa Fluor 568 goat anti-mouse IgG (red). Representative IFA images are shown. (B) On days 2, 3, and 4 p.t., culture fluids were collected and used to infect naive BHK-21 cells for viral titer quantification and viral gene sequencing. Capsid proteins in infected BHK-21 cells were detected by IFA (green). Representative IFA images are shown. (C) Intracellular viral RNAs from infected BHK-21 cells were extracted and subjected to RT-PCR and cDNA sequencing, and amino acid and nucleotide sequences are shown. (D) Capsid-positive cells from the IFA data (B) were counted. Average viral titers (IFU/ml) from triplicate samples are shown.

DISCUSSION

The goal of this study was to characterize the function of DENV NS2A using a mutagenesis approach. Three classes of mutants were identified (Table 1). (i) Class I mutants showed weak defects in viral replication. This class included 9 of the 16 selected residues conserved or semiconserved in flaviviruses. The moderate effect of these mutations on viral replication is surprising, since seven of the class I residues are conserved (R24, R26, T97, and K99) or identical (G46, G69, and F81) among NS2A proteins of the various flaviviruses. It should be noted that the effect of class I mutations on viral replication could be exerted through attenuation of viral RNA synthesis and/or virion assembly. (ii) Class II mutants (the D125 and G200 mutants) were defective in viral RNA synthesis, leading to a decreased production of viral particles. The class II

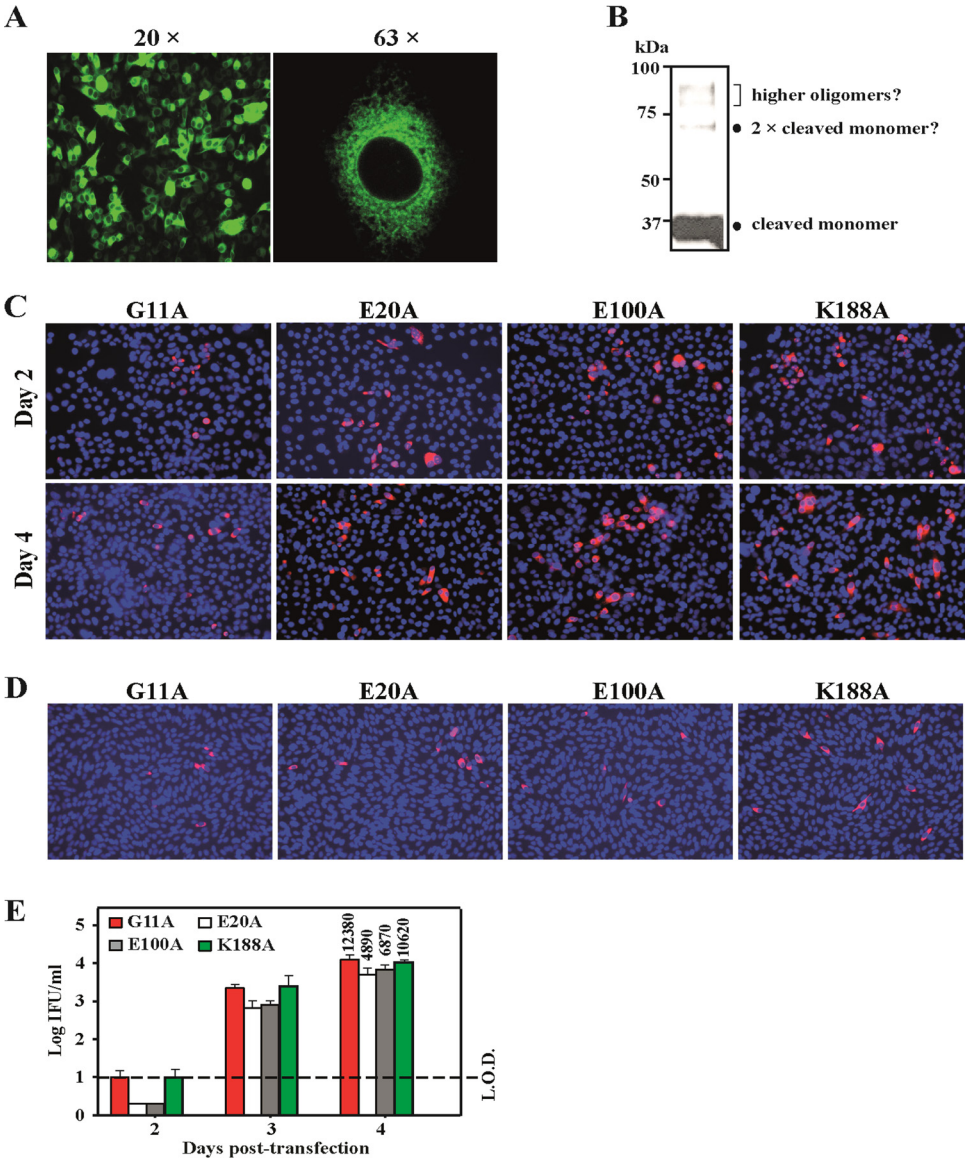

FIG 8 *trans*-Complementation analysis using NS2A (G200A)-EGFP BHK-21 cells. (A) Characterization of NS2A (G200A)-EGFP BHK-21 cells by IFA. EGFP fusion proteins probed by a mouse anti-EGFP IgG (green) are shown. (B) Western blot analysis. EGFP fusion proteins in BHK-21-NS2A (G200A)-EGFP cells were precipitated and detected by Western blotting using EGFP antibodies. Equal amounts of class III mutant genome-length RNAs were electroporated into NS2A (G200A)-EGFP BHK-21 cells. (C) On days 2 and 4 p.t., E proteins were examined by IFA. Representative images are shown. (D) Culture fluids collected on days 2, 3, and 4 p.t. were used to infect naive BHK-21 cells. IFA was performed using D2C1 antibody and Alexa Fluor 568 goat anti-mouse IgG (red). Representative images are shown. (E) Virus titers. The limit of detection (L.O.D.) was 10 IFU/ml.

mutations are not likely to affect virion assembly because the supply of the class II mutant NS2A protein (G200A) in *trans* could efficiently rescue the defect in virion assembly of the class III mutants. (iii) Class III mutants (the G11A, E20A, E100A, Q187A, and K188A mutants) were competent in viral RNA synthesis but incompetent in virion assembly. Our results are in agreement with previous reports that flavivirus NS2A functions in both viral RNA synthesis and virion assembly (8, 22, 28, 29). Figure 1A summarizes the locations of the three classes of mutations on a DENV-2 NS2A membrane topology model (22). Residues from each mutant class are not clustered to any specific regions on this two-dimensional NS2A model. A three-dimensional crystal structure is required to illuminate how residues from each mutant class are spatially related to each other.

Flavivirus NS2A is essential for viral RNA synthesis. Kunjin virus NS2A was reported to colocalize with dsRNA, NS3, and NS5 in vesicle packets (27). Vesicle packets are sites where the replication complexes reside. It is currently unclear how NS2A participates in viral RNA synthesis. Among the two class II mutants, we showed that the D125A mutation abolished viral RNA synthesis through blocking cleavage at the NS1-NS2A junction. Alternative replacement of Asp125 with Asn (D125N) or Pro (D125P) also blocked the N-terminal cleavage of NS2A. The uncleaved NS1-NS2A might abolish viral RNA synthesis through two possible means. (i) The NS1-NS2A fusion protein may alter the conformation of NS2A and thus prevent its interactions with other viral and host factors, leading to a loss of viral RNA synthesis. (ii) The uncleaved NS1-NS2A might attenuate the function of NS1, which is

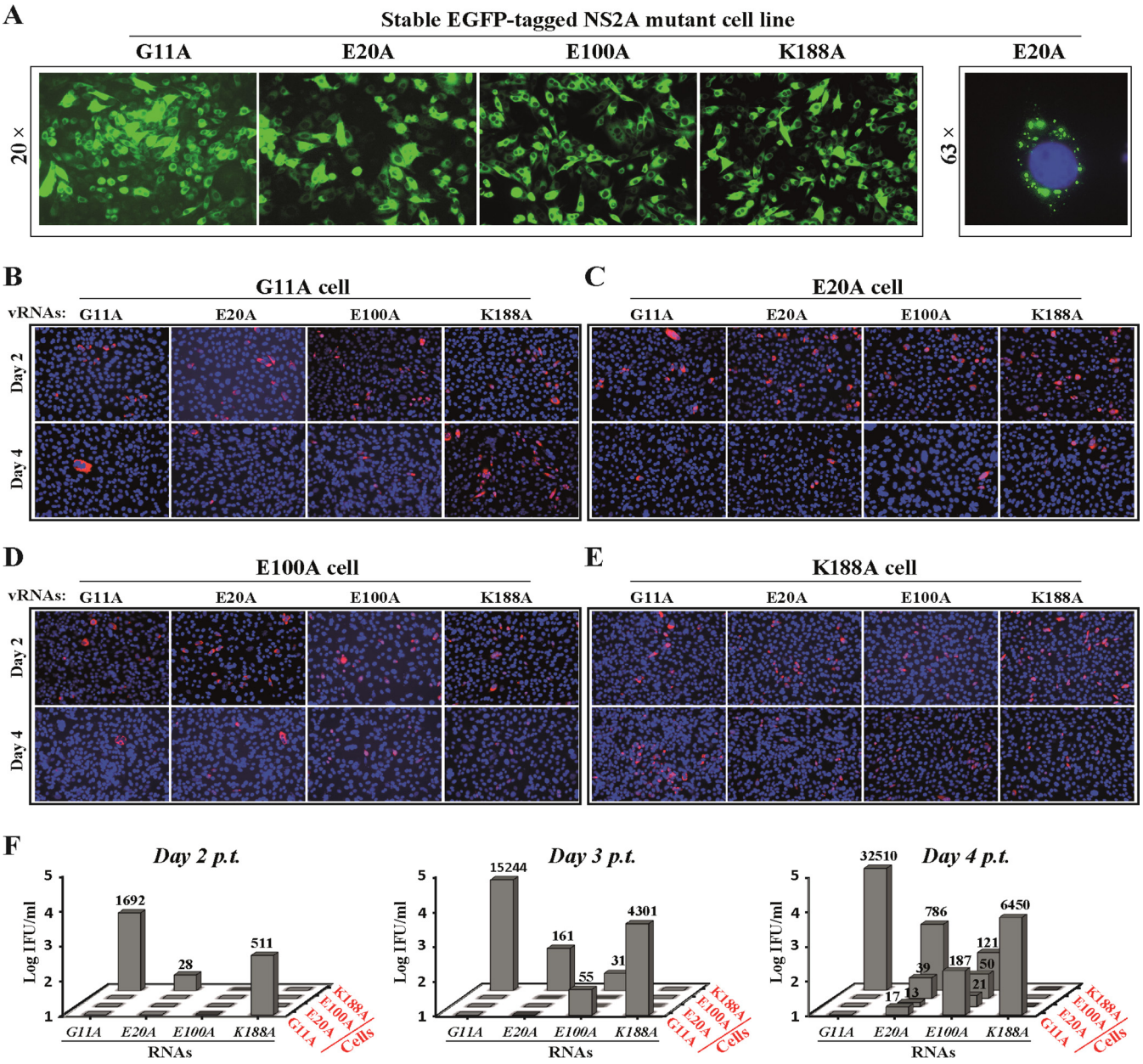

FIG 9 *trans*-Complementation analysis using cells electroporated with class III mutant NS2A-EGFP. (A) Characterization of stable cells by IFA using EGFP antibodies. Nuclei stained by DAPI are blue. Cells were electroporated with individual class III mutant G11A, E20A, E100A, and K188A RNAs. On days 2 and 4 p.t., E proteins were analyzed by IFA. (B to E) Images of cells electroporated with mutant G11A (B), E20A (C), E100A (D), and K188A (E) RNAs. Extracellular viruses in the culture fluids harvested on days 2, 3, and 4 p.t. were quantified by IFA using D2C1 antibodies. (F) Summary of viral titers. Average results for duplicate samples are shown.

essential for viral RNA synthesis (5). Mechanistically, it is intriguing to ask how mutation of the D residue at position 125, located far downstream of the N-terminal cleavage site of NS2, could abolish NS1-NS2A cleavage. A crystal structure of DENV NS2A is required to illustrate whether residue D125 is positioned close to the NS1-NS2A cleavage junction; if this is the case, the D125A mutation may affect host protease recognition of the NS1-NS2A junction. Notably, our data contradict those of a previous study showing that a mutant with a D124N mutation in DENV-4 NS2A (corresponding to D125A of DENV-2 NS2A in this study) retained about 50% of the WT NS1-NS2A cleavage efficiency when the fusion protein was translated in *vitro* (23). This discrepancy could be caused by the different experimental systems used: *in vitro* translation/cleavage in the previous study (23) versus translation/cleavage inside cells in the current study. Alternatively, the discrepancy could be due to the different serotypes of DENV analyzed in these two studies. As indicated by the amino acid sequence alignment (Fig. 1B), D125 is a conserved but not identical residue among flaviviruses (Asn is found at the same position in DENV-3, JEV, WNV, and YFV). Care should be taken when extrapolating the current result to other flaviviruses.

In contrast to the D125A mutation, the NS2A G200A substitu-

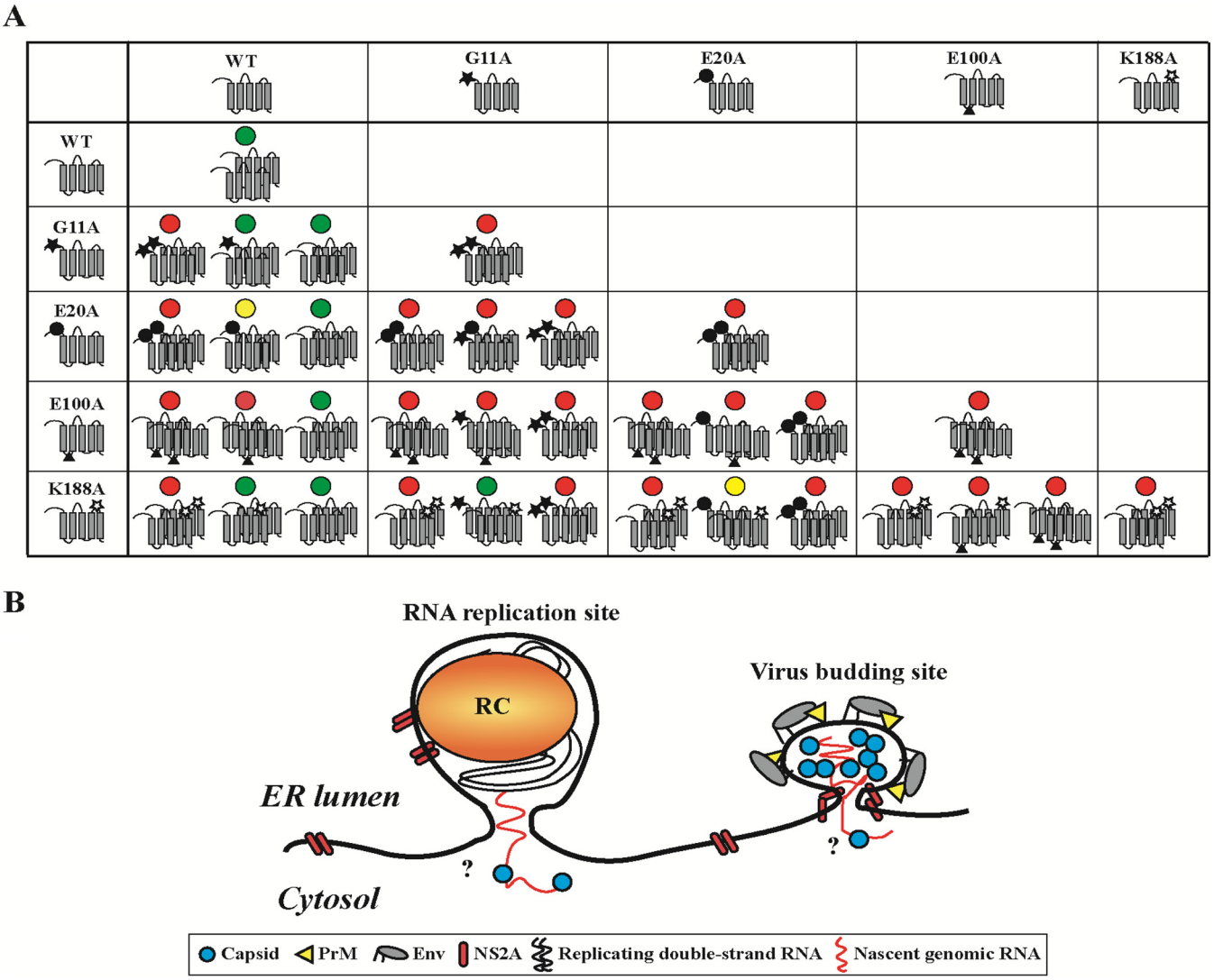

FIG 10 Two sets of NS2A molecules are responsible for DENV RNA synthesis and virion assembly. (A) Schematic diagram of *trans*-complementation. Heterogeneous combinations of NS2A mutants result in three different oligomer species. Red, yellow, and green dots indicate oligomers with no complementation and a low and a high efficiency of complementation, respectively. See the text for a detailed explanation. (B) Model of the NS2A distribution in the replication complexes (RC) and virus budding site at the ER membrane. Nascent RNAs produced by the replication complex (enclosed in the virus-induced membrane vesicle) are transported to the virus budding site for encapsidation and envelope formation. NS2A in the replication complex could be derived only in *cis*; the vesicle-compartmentalized NS2A molecules are not exchangeable with those outside the replication complex. NS2A proteins distributed around the virus budding site coordinate the encapsidation of nascent genomic RNA with capsid protein, followed by envelope formation; these NS2A proteins are readily exchangeable with other NS2A molecules.

tion showed no effect on the N-terminal cleavage of NS2A and was lethal for viral RNA synthesis, indicating that the G200A mutation abolishes viral RNA synthesis through a mechanism that is different from that for the D125A mutation. Since amino acid G200 is located in the last transmembrane segment of NS2A (Fig. 1A), this substitution might affect the local conformation of the transmembrane segment, leading to a weakened interaction between NS2A and other viral/host proteins in the replication complex. Our attempts to identify an NS2A-binding partner(s) through revertant analysis of the G200A mutant failed; in multiple experiments, the G200A mutation rapidly reverted to the WT G200 without any change at a second site (Fig. 3C, 5E, and 7C).

Assembly of infectious flavivirus particles is a complex process requiring encapsidation of the nucleocapsid into an enveloped membrane associated with the prM and E proteins. It has been proposed that flavivirus assembly occurs at a putative budding site at the ER in close proximity to the virus-induced membrane vesicles, where the replication complexes reside (33–35). Until now, NS2A and NS3 are the only two nonstructural proteins that have been reported to directly engage in flavivirus assembly (8, 22, 28, 29). NS1 might indirectly participate in virion assembly (36). The current study has identified five NS2A residues (class III) that are critical for virion assembly; the virion assembly defect observed with these class III mutants is not due to their mutational effect on viral RNA synthesis, as evidenced by the robust replication of the mutant replicons (Fig. 4). Similar to these results, Kummerer and Rice previously showed that YFV NS2A K190S (corresponding to residue K188 in DENV-2 NS2A, as shown Fig. 1A) was important

for virion assembly; in addition, they found that a genetic interaction between NS2A and NS3 was essential for YFV assembly (28). During virion assembly, these NS2A residues might participate in viral/host protein-protein interactions to orchestrate viral RNA encapsidation and membrane envelope formation. We are currently performing revertant analysis of the class III mutants to search for a potential viral protein(s) that interacts with NS2A during virion assembly.

Complementation analysis showed that NS2A mutants defective in viral RNA synthesis (class II) could not be rescued by the supply in *trans* of the wild-type NS2A from a replicon or NS2A protein alone. These results have two implications. (i) Functional NS2A in the replication complex should be provided in *cis*. Upon flavivirus RNA translation, the NS4A protein induces rearrangement of the ER membrane to form a compartment to enclose the replication complex (37). Since Kunjin virus NS2A was shown to directly bind to the NS4A protein (27), the NS2A/NS4A interaction might be a driving force to recruit NS2A to the replication complex in the RNA synthesis compartment. (ii) Once the replication complex is formed, the NS2A protein is not exchangeable with other NS2A molecules. Such restriction could be due to the compartmentalization of the replication complex.

In stark contrast to the class II mutants, class III NS2A mutants (defective in virion assembly) could be rescued by the supply in *trans* of the WT NS2A from the replicon, a WT NS2A protein expressed alone, a class II mutant NS2A (G200A is lethal for viral RNA synthesis), or a distinct class III mutant NS2A. As observed in this study, NS2A probably forms oligomers intracellularly (Fig. 6D and 8B). Direct proof of NS2A oligomerization in infected cells is currently difficult due to a lack of NS2A antibodies. The current resolution does not allow us to conclude how and what type of NS2A oligomers contribute to virion assembly. However, the putative oligomerization of the NS2A protein could be responsible for the *trans*-complementation (Fig. 10A). For example, when G11A NS2A cells are transfected with K188A mutant RNA, three species of NS2A oligomers could potentially be formed: a G11A-G11A oligomer, a K188A-K188A oligomer, or a G11A-K188A oligomer. Among these, only the G11A-K188A oligomer may function in virion assembly. However, it should be noted that not all combinations of the class III NS2A mutants could be successfully complemented. The efficiency of *trans*-complementation is likely determined by the mechanistic defects of the two mutations. Nevertheless, these results clearly indicate that the NS2A molecules required for virion assembly are exchangeable with other NS2A proteins. It should be noted that the current study was performed in mammalian cells. Future experiments are needed to examine whether similar results could be obtained in mosquito cells.

Collectively, our findings support a model in which two distinct sets of NS2A molecules are responsible for viral RNA synthesis and virion assembly (Fig. 10B). One set of NS2A molecules is located in the replication complex for RNA synthesis; another set of NS2A molecules is located in the virus budding site for virion assembly. Since Kunjin virus NS2A has been reported to bind to viral RNA (27), flavivirus NS2A may function as a transporter to transfer nascent genomic RNA synthesized from the replication complex to the virion assembly site (38). The molecular details of the interplay among NS2A, NS3, three structural proteins, genomic RNA, and host factors remain to be defined.

ACKNOWLEDGMENTS

We thank colleagues at the Novartis Institute for Tropical Diseases for helpful discussion and support during the course of this work.

This project was partially supported by the TCR flagship STOP Dengue program from the National Medical Research Council in Singapore to NITD.

REFERENCES

1. **Lindenbach BD, Thiel H-J, Rice CM.** 2007. Flaviviridae: the viruses and their replication, p 1101–1152. *In* Knipe DM, Howley PM, Griffin DE, Lamb RA, Martin MA, Roizman B, Straus SE (ed), Fields virology, 5th ed, vol 1. Lippincott Williams & Wilkins, Philadelphia, PA.
2. **Bhatt S, Gething PW, Brady OJ, Messina JP, Farlow AW, Moyes CL, Drake JM, Brownstein JS, Hoen AG, Sankoh O, Myers MF, George DB, Jaenisch T, Wint GR, Simmons CP, Scott TW, Farrar JJ, Hay SI.** 2013. The global distribution and burden of dengue. Nature **496:**504–507. http://dx.doi.org/10.1038/nature12060.
3. **Hahn YS, Galler R, Hunkapiller T, Dalrymple JM, Strauss JH, Strauss EG.** 1988. Nucleotide sequence of dengue 2 RNA and comparison of the encoded proteins with those of other flaviviruses. Virology **162:**167–180. http://dx.doi.org/10.1016/0042-6822(88)90406-0.
4. **Westaway EG, Mackenzie JM, Kenney MT, Jones MK, Khromykh AA.** 1997. Ultrastructure of Kunjin virus-infected cells: colocalization of NS1 and NS3 with double-stranded RNA, and of NS2B with NS3, in virus-induced membrane structures. J Virol **71:**6650–6661.
5. **Lindenbach BD, Rice CM.** 1997. *trans*-Complementation of yellow fever virus NS1 reveals a role in early RNA replication. J Virol **71:**9608–9617.
6. **Warrener P, Tamura JK, Collett MS.** 1993. RNA-stimulated NTPase activity associated with yellow fever virus NS3 protein expressed in bacteria. J Virol **67:**989–996.
7. **Wengler G, Czaya G, Farber PM, Hegemann JH.** 1991. In vitro synthesis of West Nile virus proteins indicates that the amino-terminal segment of the NS3 protein contains the active centre of the protease which cleaves the viral polyprotein after multiple basic amino acids. J Gen Virol **72**(Pt 4)**:**851–858. http://dx.doi.org/10.1099/0022-1317-72-4-851.
8. **Patkar CG, Kuhn RJ.** 2008. Yellow fever virus NS3 plays an essential role in virus assembly independent of its known enzymatic functions. J Virol **82:**3342–3352. http://dx.doi.org/10.1128/JVI.02447-07.
9. **Dong H, Chang DC, Hua MH, Lim SP, Chionh YH, Hia F, Lee YH, Kukkaro P, Lok SM, Dedon PC, Shi PY.** 2012. 2′-O methylation of internal adenosine by flavivirus NS5 methyltransferase. PLoS Pathog **8:**e1002642. http://dx.doi.org/10.1371/journal.ppat.1002642.
10. **Egloff MP, Benarroch D, Selisko B, Romette JL, Canard B.** 2002. An RNA cap (nucleoside-2′-O-)-methyltransferase in the flavivirus RNA polymerase NS5: crystal structure and functional characterization. EMBO J **21:**2757–2768. http://dx.doi.org/10.1093/emboj/21.11.2757.
11. **Ray D, Shah A, Tilgner M, Guo Y, Zhao Y, Dong H, Deas TS, Zhou Y, Li H, Shi PY.** 2006. West Nile virus 5′-cap structure is formed by sequential guanine N-7 and ribose 2′-O methylations by nonstructural protein 5. J Virol **80:**8362–8370. http://dx.doi.org/10.1128/JVI.00814-06.
12. **Issur M, Geiss BJ, Bougie I, Picard-Jean F, Despins S, Mayette J, Hobdey SE, Bisaillon M.** 2009. The flavivirus NS5 protein is a true RNA guanylyltransferase that catalyzes a two-step reaction to form the RNA cap structure. RNA **15:**2340–2350. http://dx.doi.org/10.1261/rna.1609709.
13. **Ackermann M, Padmanabhan R.** 2001. De novo synthesis of RNA by the dengue virus RNA-dependent RNA polymerase exhibits temperature dependence at the initiation but not elongation phase. J Biol Chem **276:**39926–39937. http://dx.doi.org/10.1074/jbc.M104248200.
14. **Miller S, Kastner S, Krijnse-Locker J, Buhler S, Bartenschlager R.** 2007. The non-structural protein 4A of dengue virus is an integral membrane protein inducing membrane alterations in a 2K-regulated manner. J Biol Chem **282:**8873–8882. http://dx.doi.org/10.1074/jbc.M609919200.
15. **Zou J, Xie X, Lee LT, Chandrasekaran R, Reynaud A, Yap L, Wang QY, Dong H, Kang C, Yuan Z, Lescar J, Shi PY.** 2014. Dimerization of flavivirus NS4B protein. J Virol **88:**3379–3391. http://dx.doi.org/10.1128/JVI.02782-13.
16. **Miller S, Sparacio S, Bartenschlager R.** 2006. Subcellular localization and membrane topology of the dengue virus type 2 non-structural protein 4B. J Biol Chem **281:**8854–8863. http://dx.doi.org/10.1074/jbc.M512697200.
17. **Ashour J, Laurent-Rolle M, Shi PY, Garcia-Sastre A.** 2009. NS5 of dengue virus mediates STAT2 binding and degradation. J Virol **83:**5408–5418. http://dx.doi.org/10.1128/JVI.02188-08.

18. **Laurent-Rolle M, Boer EF, Lubick KJ, Wolfinbarger JB, Carmody AB, Rockx B, Liu W, Ashour J, Shupert WL, Holbrook MR, Barrett AD, Mason PW, Bloom ME, Garcia-Sastre A, Khromykh AA, Best SM.** 2010. The NS5 protein of the virulent West Nile virus NY99 strain is a potent antagonist of type I interferon-mediated JAK-STAT signaling. J Virol **84:** 3503–3515. http://dx.doi.org/10.1128/JVI.01161-09.
19. **Morrison J, Laurent-Rolle M, Maestre AM, Rajsbaum R, Pisanelli G, Simon V, Mulder LC, Fernandez-Sesma A, Garcia-Sastre A.** 2013. Dengue virus co-opts UBR4 to degrade STAT2 and antagonize type I interferon signaling. PLoS Pathog **9:**e1003265. http://dx.doi.org/10.1371/journal.ppat.1003265.
20. **Munoz-Jordan JL, Laurent-Rolle M, Ashour J, Martinez-Sobrido L, Ashok M, Lipkin WI, Garcia-Sastre A.** 2005. Inhibition of alpha/beta interferon signaling by the NS4B protein of flaviviruses. J Virol **79:**8004–8013. http://dx.doi.org/10.1128/JVI.79.13.8004-8013.2005.
21. **Munoz-Jordan JL, Sanchez-Burgos GG, Laurent-Rolle M, Garcia-Sastre A.** 2003. Inhibition of interferon signaling by dengue virus. Proc Natl Acad Sci U S A **100:**14333–14338. http://dx.doi.org/10.1073/pnas.2335168100.
22. **Xie X, Gayen S, Kang C, Yuan Z, Shi PY.** 2013. Membrane topology and function of dengue virus NS2A protein. J Virol **87:**4609–4622. http://dx.doi.org/10.1128/JVI.02424-12.
23. **Falgout B, Markoff L.** 1995. Evidence that flavivirus NS1-NS2A cleavage is mediated by a membrane-bound host protease in the endoplasmic reticulum. J Virol **69:**7232–7243.
24. **Liu WJ, Chen HB, Wang XJ, Huang H, Khromykh AA.** 2004. Analysis of adaptive mutations in Kunjin virus replicon RNA reveals a novel role for the flavivirus nonstructural protein NS2A in inhibition of beta interferon promoter-driven transcription. J Virol **78:**12225–12235. http://dx.doi.org/10.1128/JVI.78.22.12225-12235.2004.
25. **Liu WJ, Wang XJ, Clark DC, Lobigs M, Hall RA, Khromykh AA.** 2006. A single amino acid substitution in the West Nile virus nonstructural protein NS2A disables its ability to inhibit alpha/beta interferon induction and attenuates virus virulence in mice. J Virol **80:**2396–2404. http://dx.doi.org/10.1128/JVI.80.5.2396-2404.2006.
26. **Tu YC, Yu CY, Liang JJ, Lin E, Liao CL, Lin YL.** 2012. Blocking double-stranded RNA-activated protein kinase PKR by Japanese encephalitis virus nonstructural protein 2A. J Virol **86:**10347–10358. http://dx.doi.org/10.1128/JVI.00525-12.
27. **Mackenzie JM, Khromykh AA, Jones MK, Westaway EG.** 1998. Subcellular localization and some biochemical properties of the flavivirus Kunjin nonstructural proteins NS2A and NS4A. Virology **245:**203–215. http://dx.doi.org/10.1006/viro.1998.9156.
28. **Kummerer BM, Rice CM.** 2002. Mutations in the yellow fever virus nonstructural protein NS2A selectively block production of infectious particles. J Virol **76:**4773–4784. http://dx.doi.org/10.1128/JVI.76.10.4773-4784.2002.
29. **Leung JY, Pijlman GP, Kondratieva N, Hyde J, Mackenzie JM, Khromykh AA.** 2008. Role of nonstructural protein NS2A in flavivirus assembly. J Virol **82:**4731–4741. http://dx.doi.org/10.1128/JVI.00002-08.
30. **Puttikhunt C, Ong-Ajchaowlerd P, Prommool T, Sangiambut S, Netsawang J, Limjindaporn T, Malasit P, Kasinrerk W.** 2009. Production and characterization of anti-dengue capsid antibodies suggesting the N terminus region covering the first 20 amino acids of dengue virus capsid protein is predominantly immunogenic in mice. Arch Virol **154:**1211–1221. http://dx.doi.org/10.1007/s00705-009-0426-5.
31. **Xie X, Wang QY, Xu HY, Qing M, Kramer L, Yuan Z, Shi PY.** 2011. Inhibition of dengue virus by targeting viral NS4B protein. J Virol **85:**11183–11195. http://dx.doi.org/10.1128/JVI.05468-11.
32. **Zou G, Zhang B, Lim PY, Yuan Z, Bernard KA, Shi PY.** 2009. Exclusion of West Nile virus superinfection through RNA replication. J Virol **83:**11765–11776. http://dx.doi.org/10.1128/JVI.01205-09.
33. **Welsch S, Miller S, Romero-Brey I, Merz A, Bleck CK, Walther P, Fuller SD, Antony C, Krijnse-Locker J, Bartenschlager R.** 2009. Composition and three-dimensional architecture of the dengue virus replication and assembly sites. Cell Host Microbe **5:**365–375. http://dx.doi.org/10.1016/j.chom.2009.03.007.
34. **Junjhon J, Pennington JG, Edwards TJ, Perera R, Lanman J, Kuhn RJ.** 2014. Ultrastructural characterization and three-dimensional architecture of replication sites in dengue virus-infected mosquito cells. J Virol **88:**4687–4697. http://dx.doi.org/10.1128/JVI.00118-14.
35. **Gillespie LK, Hoenen A, Morgan G, Mackenzie JM.** 2010. The endoplasmic reticulum provides the membrane platform for biogenesis of the flavivirus replication complex. J Virol **84:**10438–10447. http://dx.doi.org/10.1128/JVI.00986-10.
36. **Winkelmann ER, Widman DG, Suzuki R, Mason PW.** 2011. Analyses of mutations selected by passaging a chimeric flavivirus identify mutations that alter infectivity and reveal an interaction between the structural proteins and the nonstructural glycoprotein NS1. Virology **421:**96–104. http://dx.doi.org/10.1016/j.virol.2011.09.007.
37. **Roosendaal J, Westaway EG, Khromykh A, Mackenzie JM.** 2006. Regulated cleavages at the West Nile virus NS4A-2K-NS4B junctions play a major role in rearranging cytoplasmic membranes and Golgi trafficking of the NS4A protein. J Virol **80:**4623–4632. http://dx.doi.org/10.1128/JVI.80.9.4623-4632.2006.
38. **Liu WJ, Chen HB, Khromykh AA.** 2003. Molecular and functional analyses of Kunjin virus infectious cDNA clones demonstrate the essential roles for NS2A in virus assembly and for a nonconservative residue in NS3 in RNA replication. J Virol **77:**7804–7813. http://dx.doi.org/10.1128/JVI.77.14.7804-7813.2003.